

DSI2I: Dense Style for Unpaired Image-to-Image Translation

Baran Ozaydin, Tong Zhang, Sabine Süsstrunk, Mathieu Salzmann
School of Computer and Communication Sciences, EPFL, Switzerland

{baran.ozaydin, tong.zhang, sabine.susstrunk, mathieu.salzmann}@epfl.ch

Abstract

Unpaired exemplar-based image-to-image (UEI2I) translation aims to translate a source image to a target image domain with the style of a target image exemplar, without ground-truth input-translation pairs. Existing UEI2I methods represent style using either a global, image-level feature vector, or one vector per object instance/class but requiring knowledge of the scene semantics. Here, by contrast, we propose to represent style as a dense feature map, allowing for a finer-grained transfer to the source image without requiring any external semantic information. We then rely on perceptual and adversarial losses to disentangle our dense style and content representations, and exploit unsupervised cross-domain semantic correspondences to warp the exemplar style to the source content. We demonstrate the effectiveness of our method on two datasets using standard metrics together with a new localized style metric measuring style similarity in a class-wise manner. Our results evidence that the translations produced by our approach are more diverse and closer to the exemplars than those of the state-of-the-art methods while nonetheless preserving the source content.

1. Introduction

Unpaired image-to-image (UI2I) translation aims to translate a source image to a target image domain by training a deep network using images from the source and target domains without ground-truth input-translation pairs. In the exemplar-based scenario (UEI2I), an additional target image exemplar is provided as input so as to further guide the style translation. Ultimately, the resulting translation should 1) preserve the content/semantics of the source image; 2) convincingly seem to belong to the target domain; and 3) adopt the specific style of the target exemplar image.

Existing UEI2I strategies [11, 18] encode the style of the exemplar using a global, image-level feature vector. While this has proven to be effective for relatively simple scenes, it leads to undesirable artifacts for complex, multi-object ones, as illustrated in Fig. 1, where appearance informa-

tion of the dominating semantic regions, such as sky, unnaturally bleeds into other semantic areas, such as the road, tree and buildings. Some methods [3, 12, 15, 33] address this by computing instance-wise or class-wise style representations. However, they require knowledge of the scene semantics, e.g., segmentation masks or bounding boxes during training, which limits their applicability.

Here, by contrast, we propose to model style densely. That is, we represent the style of an image with a feature tensor that has the same spatial resolution as the content one. The difficulty in doing so lies in the fact that style information can then more easily pollute the content one, and vice versa. To prevent this and encourage the disentanglement of style and content, we utilize perceptual and adversarial losses on randomly-stylized content representations, which encourages the model to preserve fidelity and semantics in the absence of a dense style component.

Dense style representation alone is not beneficial for UEI2I as spatial arrangement of each dense style component is only applicable for its own image. Hence, we propose a cross-domain semantic correspondence module to spatially arrange/warp the dense style of the target image for the source content. To that end, we utilize the vision backbone from CLIP [30] as feature extractor and find correspondence between the features of source and target images using Optimal Transport [6, 25].

As a consequence, and as shown in Fig. 1, our approach transfers the local style of the exemplar to the source content in a more natural manner than the global-style techniques. Yet, in contrast to [3, 12, 15, 33], it does not require semantic supervision during training, thanks to our dense modeling of style. To quantitatively evaluate the benefits of our approach, we introduce a metric that better reflects the stylistic similarity between the translations and the exemplars than the image-level metrics used in the literature.

Our contributions can be summarized as follows:

- We propose a dense style representation for UEI2I. Our method retains the source content in the translation while providing finer-grain stylistic control.
- We show that adversarial and perceptual losses encour-

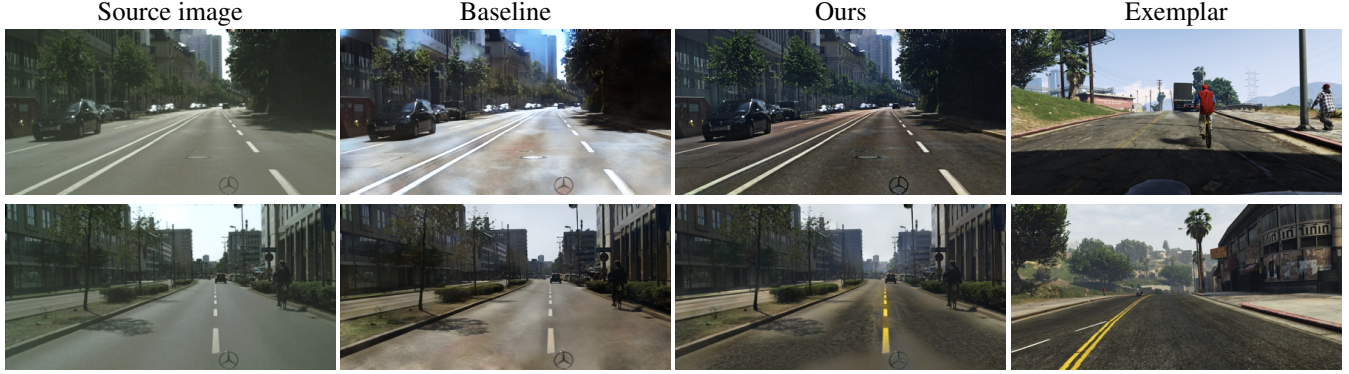


Figure 1. **Global style vs dense style representations.** The baseline method (MUNIT) [11] represents the exemplar style with a single, image-level feature vector. As such, some appearance information from the exemplar bleeds into semantically-incorrect regions, giving, for example, an unnatural bluish taint to the road and the buildings in the first row, second image. By modeling style densely, our approach better respects the semantics when applying style from the exemplar to the translated image. Our method also has finer-grained control over style. The color of the road and center line in the second row reflect exemplar appearance more accurately.

Method	No Label	Multi-modal	Exemplar guided	Local style
MUNIT [11]	✓	✓	✓	✗
DRIT [18]	✓	✓	✓	✗
CUT [28]	✓	✗	✗	✗
FSeSim [42]	✓	✓	✗	✗
MGUIT [12]	✗	✓	✓	✓
Ours	✓	✓	✓	✓

Table 1. Comparison of I2I methods.

age the disentanglement of our dense style and content representations.

- We develop a cross-domain semantic correspondence module to warp the exemplar style to the source content.
- We propose a localized style metric to measure the stylistic accuracy of the translation.

Our experiments evidence both qualitatively and quantitatively the benefits of our method over global, image-level style representations. We will make our code publicly available upon acceptance.

2. Related Work

Our method primarily relates to three lines of research: Image-to-image (I2I) translation, Style Transfer, and Semantic Correspondence. Our main source of inspiration is I2I research as it deals with content preservation and translation fidelity. However, we borrow concepts from Style Transfer when it comes to adopting exemplar style and evaluating stylistic accuracy. Furthermore, our approach to swapping styles across semantically relevant parts of different images can be related to semantic correspondence.

2.1. Image-to-image Translation

We focus the discussion of I2I methods on the unpaired scenario, as our method does not utilize paired data. CycleGAN [44] was the first work to address this by utilizing cycle consistency as a source of supervision in the presence of unpaired images from two domains. Recent works [9, 13, 28, 42] lift the cycle consistency requirement and perform one-sided translation while achieving high fidelity. To this end, they utilize contrastive losses and/or self-similarity between the source and the translation. Many I2I methods, however, are unimodal, in that they produce a single translation per input image, thus not reflecting the diversity of the target domain, especially in the presence of high within-domain variance. Although some works [13, 42] extend this to multimodal outputs, they cannot adopt the style of a specific target exemplar, which is what we address.

Some effort has nonetheless been made to develop exemplar-guided I2I methods. For example, [11, 18] decompose the images into content and style components, and generate exemplar-based translations by merging the exemplar style with the content of the source image. However, these models define a single style representation for the whole image, which does not reflect the complexity of multi-object scenes. By contrast, [3, 12, 15, 27, 33] reason about object instances for I2I translation. Their goal is thus similar to ours, but their style representations focus on foreground objects only, and they require object-level (pseudo) annotations during training. Moreover, these methods are evaluated based on object detection scores and output diversity, but they do not report how stylistically close their translations are to the exemplars. Here, we achieve dense style transfer for all categories without requiring annotations and show that our method generates translations closer

to the exemplar style while having comparable fidelity with that of state-of-the-art methods.

2.2. Style Transfer

Style transfer aims to bring the appearance of the content image closer to a target image. The seminal work of Gatys et al. [7] achieves so by matching the Gram matrices of the two images via image-based optimization. [20] provides an analytical solution to Gram matrix alignment, enabling arbitrary style transfer without image based optimization. [10] only matches the diagonal of the Gram matrices by adjusting the channel means and standard deviations. [22] shows that matching the Gram matrices minimizes the Maximum Mean Discrepancy between the two feature distributions. Inspired by this distribution interpretation, [17] proposes to minimize a relaxed Earth Movers Distance between the two distributions, showing the effectiveness of Optimal Transport in style transfer. [41] defines multiple styles per image via GrabCut and exchanges styles between the local regions in two images. [17, 41] are particularly relevant to our work as they account for the spatial aspect of style. [4, 21, 36] aim to achieve photorealistic stylization using a pre-trained VGG based autoencoder. [16, 24, 35] model texture and geometry based style separately and learn to warp the texture-based style to the geometry of another image. However, the geometric warping module they rely on makes their methods only applicable to images depicting single objects. Unlike these works, our method operates on complex scenes.

2.3. Semantic Correspondence

Semantic correspondence methods aim to find semantically related regions across two different images. This involves the challenging task of matching object parts and fine-grained keypoints. Early approaches [2, 23] used hand-crafted features for this task. These features, however, are not invariant to changes in illumination, appearance, and other low-level factors that do not affect semantics. Hence, they have limited ability to generalize across different scenes. [1, 25, 26] use ImageNet [34] pre-trained features to address this issue and find correspondence between images containing similar objects. However, these methods do not generalize to finding accurate correspondences across images from different modalities/domains.

Semantic correspondence has been explored in the context of image to image translation as well. In particular, [38–40, 43] use cross domain correspondences to guide paired exemplar-based I2I translation. In their case, both the I2I and semantic correspondence tasks benefit from the paired supervision. Here, we also use cross domain correspondences, but unlike these works, we do so for unpaired, unsupervised, and exemplar-based I2I translation.

3. Method

Let us now introduce our UEI2I approach using dense style representations. To this end, we first define the main architectural components of our model. It largely follows the architecture of [11] and is depicted in Fig 2. Given two image domains $\mathbf{X}, \mathbf{Y} \subset \mathbb{R}^{3 \times H'W'}$, our model consists of two style encoders $E_X^s, E_Y^s : \mathbb{R}^{3 \times H'W'} \rightarrow \mathbb{R}^{S \times HW}$, two content encoders $E_X^c, E_Y^c : \mathbb{R}^{3 \times H'W'} \rightarrow \mathbb{R}^{C \times HW}$, two generators $G_X, G_Y : \mathbb{R}^{C \times HW}, \mathbb{R}^{S \times HW} \rightarrow \mathbb{R}^{3 \times H'W'}$, and two patch discriminators $D_X, D_Y : \mathbb{R}^{3 \times H'W'} \rightarrow \mathbb{R}^{S \times H''W''}$.

The content and style representations are then defined as follows. The content of image \mathbf{x} is computed as $\mathbf{C}_x := E_X^c(\mathbf{x})$, and its dense style as $\mathbf{S}_x^{\text{dense}} := E_X^s(\mathbf{x})$. Note that the latter departs from the definition of style in [11]; here, instead of a global style vector, we use a dense style map, which will let us transfer style in a finer-grained manner. Nevertheless, we also compute a global style for image \mathbf{x} as $\mathbf{S}_x^{\text{global}} := \text{Expand}(\text{Avg}(\mathbf{S}_x^{\text{dense}}))$, where *Avg* denotes spatial averaging and *Expand* denotes repeating a vector across spatial dimensions. Furthermore, we define a mixed style $\mathbf{S}_x^{\text{mix}} := 0.5\mathbf{S}_x^{\text{global}} + 0.5\mathbf{S}_x^{\text{dense}}$. As will be shown later, this mixed style will allow us to preserve the content without sacrificing stylistic control.

In the remainder of this section, we first introduce our approach to injecting a dense style to produce an image. We then turn to the problem of learning meaningful dense style representations during training, shown in the top portion of Fig. 2, and finally to that of exchanging the dense styles of the source and exemplar images at inference time, illustrated in the bottom portion of Fig. 2.

3.1. Injecting Dense Style

We define style as low level attributes that do not affect the semantics of the image. These low level attributes can include lighting, color, appearance, and texture. We also believe that a change in style should not lead to an unrealistic image and should not modify the semantics of the scene. In this work, we argue that, based on this definition, style should be represented densely. Given a dense style map, $\mathbf{S}^{\text{dense}}$, extracted by one of the above-mentioned style encoders, we now describe how we inject such a representation in our framework to produce an image. Note that, in this section, we assume that the input dense style map is in direct spatial correspondence with the image content. We will explain in Section 3.3 how we handle the different spatial arrangements of the source and exemplar images.

Accurate stylization requires the removal of the existing style as an initial step [20, 22]. Thus, for our dense style to be effective, we incorporate a dense normalization that first removes the style of each region. To this end, inspired by [19, 29, 45], we utilize a Positional Normalization

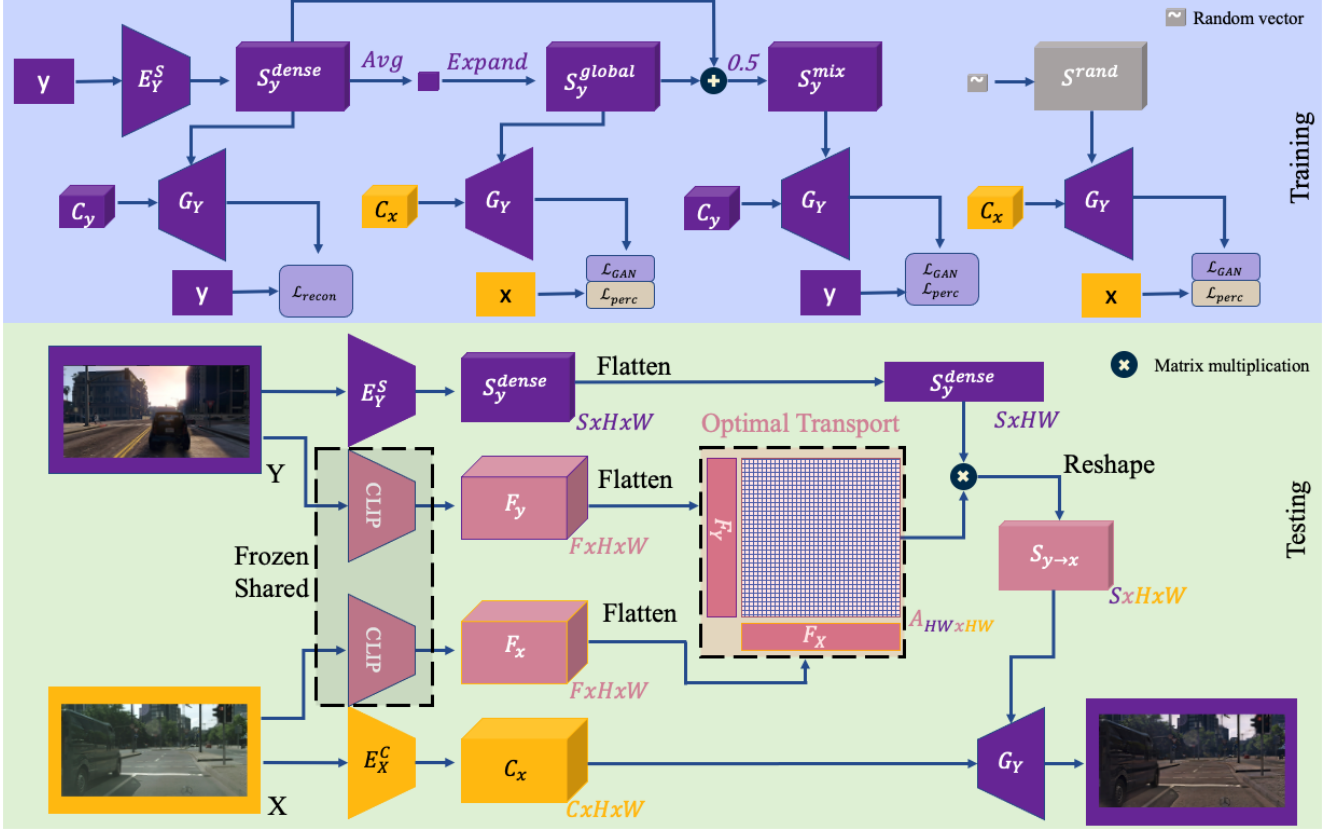


Figure 2. **Overview of our method.** During training, our method does not require any labels or paired images. During test time, we utilize CLIP backbone for building semantic correspondence. See Section 3 for definitions and explanations.

Layer [19] followed by dense modulation. These operations are performed on generator activations that produce the images.

Formally, let $\mathbf{P} \in \mathbb{R}^{C' \times HW}$ denote the generator activations, with C' the number of channels. We compute the position-wise means and standard deviations of \mathbf{P} , $\mu, \sigma \in \mathbb{R}^{HW}$. We then replace the existing style by our dense one via the Dense Normalization (DNorm) function

$$F_{DNorm}(\mathbf{P}, \alpha, \beta) = \frac{\mathbf{P} - \mu}{\sigma} \beta + \alpha \quad (1)$$

where the arithmetic operations are performed in an element-wise manner and by replicating μ and σ C' times to match the channel dimension of \mathbf{P} . The tensors $\alpha, \beta \in \mathbb{R}^{C' \times HW}$ are obtained by applying 1×1 convolutions to the dense style \mathbf{S}^{dense} .

3.2. Learning Dense Style

Let us now explain how we learn a dense style representation that accurately reflects the stylistic attributes of the exemplar. One difficulty when modeling style densely is that the image reconstruction loss will tend to encode information that goes beyond our style definition in it. To prevent

this, we utilize perceptual and adversarial losses to regularize our dense style representation. Specifically, we use the reconstruction loss

$$L_{recon} = L_1(G_Y(C_Y, \mathbf{S}_Y^{dense}), \mathbf{y}) \quad (2)$$

to let \mathbf{S}^{dense} model spatially rich and dense information. In order to prevent style from modeling content, we constrain the translations to be realistic and to preserve the semantics of the source using

$$L_{adv_global} = L_{GAN}(G_Y(C_x, \mathbf{S}_y^{global}), D_Y), \quad (3)$$

$$L_{adv_mix} = L_{GAN}(G_X(C_x, \mathbf{S}_x^{mix}), D_X), \quad (4)$$

$$L_{per_global} = L_1(VGG(\mathbf{x}), VGG(G_Y(C_x, \mathbf{S}_y^{global}))), \quad (5)$$

$$L_{per_mix} = L_1(VGG(\mathbf{x}), VGG(G_X(C_x, \mathbf{S}_x^{mix}))), \quad (6)$$

where L_{GAN} denotes a standard adversarial loss, and $VGG()$ represents the VGG16 backbone up to the the Global Average Pooling layer (exclusive). Note that adversarial and perceptual losses involve \mathbf{S}^{mix} and \mathbf{S}^{global} but not directly \mathbf{S}^{dense} ; involving \mathbf{S}^{dense} in the adversarial and

perceptual losses tends to make the model learn to ignore the style representation. Moreover, exchanging dense style across two images requires building semantic correspondence between them to warp the style of the exemplar for the source. Thus, in order to avoid a collapsed style representation and using semantic information during training, we only exchange global styles across domains and constrain reconstructions with S^{mix} . This circumvents the spatial arrangement mismatch between the source and exemplar images mentioned in Section 3.1, thus letting us directly use F_{DNorm} for dense style injection.

In addition to the above-mentioned losses, we use perceptual and GAN losses with random global style. We have observed them to encourage the model to preserve content in the absence of dense style representation. Moreover, as discussed in [11, 14], GAN loss helps matching the random latent style with the stylistic variety in the image domain.

3.3. Exchanging Dense Style

Up to now, we have discussed how to inject dense style in an image and how to learn a meaningful dense style representation in training stage. However, one problem remains unaddressed in the test stage: The dense style extracted from an image is only applicable to that same image because its spatial arrangement corresponds to that image. In this section, we therefore propose an approach to swapping dense style maps across two images from different domains.

Our approach is motivated by the intuition that style should be exchanged between semantically similar regions in both images. To achieve this, we leverage an auxiliary pre-trained network that generalizes well across various image modalities [30]. Specifically, we extract middle layer features $F_x, F_y \in \mathbb{R}^{F \times HW}$ by passing the source and exemplar images through the CLIP-RN50 backbone [30]. We then compute the cosine similarity between these features, clipping the negative similarity values to zero. We denote this matrix as Z_{yx} and use it to solve an optimal transport problem as described in [25, 40]. We construct our cost matrix C as

$$Z_{yx} = \max(\cos(F_y, F_x), 0), \quad (7)$$

$$C = 1 - Z_{yx}. \quad (8)$$

Thus, we use Sinkhorn’s Algorithm [6] to compute a doubly stochastic optimal transportation matrix $A_{yx} \in \mathbb{R}^{HW \times HW}$:

$$A_{yx} = \arg \min_A \langle A, C \rangle_F - \lambda h(A) \quad (9)$$

$$\text{s.t. } A \mathbf{1}_{HW} = p_y, \quad A^T \mathbf{1}_{HW} = p_x \quad (10)$$

where $h(A)$ denotes the entropy of A and λ is the entropy regularization parameter. $p_x, p_y \in \mathbb{R}^{HW \times 1}$ are the constraints on the row and column sums of A_{yx} . The novelty

of our semantic correspondence module lies in the way we choose the masses p_x and p_y .

The most straightforward choice for transportation masses p_x and p_y is the uniform distribution. However, doing so transports equal mass from every location in the images. This is problematic for us because we can see in Fig. 1 that when translation pairs have unbalanced classes, the largest semantic region can dominate the style representation and lead to undesired artifacts. In our example in Fig. 1, the content image expects to receive style vectors for roads, buildings, and tree but the exemplar image provides style for sky and road. This results in building and tree regions being stylized by sky attributes.

To solve the unbalanced class problem, we first assume that segmentation labels $M_x, M_y \in \{0, 1\}^{K \times HW}$ for K classes are available. We define M^k as the binary mask for the k -th class. The number of pixels in class k is defined as $\tilde{M}^k := \sum_l M^{k,l}$ where l indexes the spatial dimension. We, then, define $\hat{M}_{yy}, \hat{M}_{yx} \in \mathbb{R}^{K \times HW}$ as

$$\hat{M}_{yy} = M_y^T \tilde{M}_y \quad \text{and} \quad \hat{M}_{yx} = M_y^T \tilde{M}_x \quad (11)$$

where $\tilde{M} \in \mathbb{R}^{K \times 1}$ is the concatenation of \tilde{M}^k . We propose dividing the transportation mass p_y of each semantic region in y by the area of that semantic region to normalize the style based on class distribution of y . We also multiply the mass of each semantic region in y by the area of the same semantic class in x to match the expectations of x . We set p_x to be the uniform distribution.

$$\hat{p}_y = \frac{\hat{M}_{yx}}{\hat{M}_{yy}} \quad (12)$$

However, we perform correspondence only during test time and we cannot rely on labels. Hence, we do not know the area of any of the classes. To that end, propose estimating \hat{M}_{yy} and \hat{M}_{yx} based on features F_x and F_y . As such, we define Z_{xx} as self-similarity of x similarly to Z_{yx} and estimate a semantic area for each region in x and y as

$$R_{yy} = \sum_l Z_{yy}^l \quad \text{and} \quad R_{yx} = \sum_l Z_{yx}^l \quad (13)$$

where $Z^l \in \mathbb{R}^{1 \times HW}$ and l indexes to the second dimension of Z . We then compute \hat{p}_y as

$$\hat{p}_y = \frac{R_{yx}}{R_{yy}} \quad (14)$$

which is linearly scaled to obtain a probability distribution \hat{p}_y . Lastly, we compute A_{yx} as to warp S_y^{dense} as

$$S_{y \rightarrow x} = \text{Reshape}(S_y^{dense} A_{yx}). \quad (15)$$

With this operation, each spatial element $S_{y \rightarrow x}[h, w]$ can be seen as a weighted sum of spatial elements of $S_y^{dense}[h', w']$

with the weights being proportional to the semantic similarity between $\mathbf{F}_x^{h,w}$ and $\mathbf{F}_y^{h',w'}$. Hence, we can trade the style across semantically similar regions. Note that this can also be thought of as an attention mechanism across two images with the queries being \mathbf{F}_x , the keys \mathbf{F}_y and the values \mathbf{S}_y^{dense} .

4. Experiments

4.1. Evaluation Metrics

The current evaluation metrics in I2I do not take the spatial aspect of style into account. Hence, we propose a novel metric to evaluate the performance of our method. To that end, we use VGG until its first pooling layer, denoted as VGG , to extract features of size $\mathbb{R}^{V \times HW}$ from the input image \mathbf{x} , exemplar \mathbf{y} , and translation $\mathbf{x} \rightarrow \mathbf{y}$. Our metric uses segmentation masks to compute the style similarity across corresponding classes. Using the segmentation masks as \mathbf{M}_x^k , we compute the Gram matrix \mathbf{Q}_x^k for class k in image \mathbf{x} as

$$\mathbf{Q}_x^k = \frac{1}{\sum_l \mathbf{M}_x^{k,l}} (VGG(\mathbf{x}) \odot \mathbf{M}_x^k) (VGG(\mathbf{x}) \odot \mathbf{M}_x^k)^T. \quad (16)$$

This operation is equivalent to treating each class as a separate image and computing their Gram matrices.

We then compute the distance between the Gram matrices of corresponding classes in two images, i.e.,

$$\mathbf{L}^k(\mathbf{x}, \mathbf{y}) = \frac{1}{\mathbf{M}} \|\mathbf{Q}_x^k - \mathbf{Q}_y^k\|_F^2. \quad (17)$$

Note that $\mathbf{L}^k(\mathbf{x}, \mathbf{y})$ denotes the Maximum Mean Discrepancy (MMD) between the features of the masked regions with a degree 2 polynomial kernel [22]. Since this distance is computed based on early layer VGG features, it implies a stylistic distance between the two images [7].

However, $\mathbf{L}^k(\mathbf{x}, \mathbf{y})$ is not very informative as its scale depends on the input image pair \mathbf{x}, \mathbf{y} . Hence, we propose a metric that takes \mathbf{x} , \mathbf{y} , and $\mathbf{x} \rightarrow \mathbf{y}$ at the same time for better interpretability. We express it as

$$\mathbf{H}^k(\mathbf{x}, \mathbf{y}, \mathbf{x} \rightarrow \mathbf{y}) = \frac{\mathbf{L}^k(\mathbf{x} \rightarrow \mathbf{y}, \mathbf{y})}{\mathbf{L}^k(\mathbf{x}, \mathbf{y})} \mathbb{1}_{\{\tilde{\mathbf{M}}_x^k > 0\}} \mathbb{1}_{\{\tilde{\mathbf{M}}_y^k > 0\}}, \quad (18)$$

where $\mathbb{1}_{\{\cdot\}}$ is the indicator function.

Unlike \mathbf{L}^k , \mathbf{H}^k is more interpretable because its value would be equal to one if the translation output the content image. In an ideal translation scenario, we would expect the feature distributions of the translation and exemplar to be close to each other [17]. Hence, we would expect small values for more successful translations.

Method	Ours	MUNIT	DRIT	CUT	FSeSim	MGUIT
Number of votes	1062	861	541	166	219	15
Ratio of votes	0.35	0.28	0.18	0.05	0.07	0.05

Table 2. User study on similarity of translations with exemplars.

Along with our metric, we report the standard Inception Score (IS) [32], Conditional Inception Score (CIS) [11] and Frechet Inception Distance (FID) [8]. We also report the accuracy of a segmentation model pre-trained on the target domain and tested on source translations.

4.2. Implementation Details

We evaluate our model on the GTAV [31] and Cityscapes [5] datasets. Images from both datasets are resized to have a short side of 256. We borrow most of the hyperparameters from [11] but we scale all the adversarial losses by half since our method receives gradients from three adversarial losses for one source image. We do not change the hyperparameters for the perceptual losses. The entropy regularization term in Sinkhorn’s Algorithm in Eq. 10 is set to 0.05. During training of the I2I methods, we crop the center 224x224 pixels of the images. We report single scale evaluation with the same resolution for all the metrics. We use a pre-trained DRN [37] to report the segmentation results.

4.3. Results

Firstly, we evaluate the stylistic distance between exemplars and translations using our metric \mathbf{H}^k that we propose. We report this metric for the most frequent six classes from GTA [31] and Cityscapes [5] datasets because they co-occur in pairs of images. The trend with other classes is similar and can be seen in our supplementary material. Our method outperforms the baselines in synthetic to real and real to synthetic scenarios as shown in Table 3. Modeling style densely is effective at bringing the style of the regions closer to each other.

We then evaluate the fidelity of the translations using FID [8] in Table 4. Our method can generate translations with high fidelity. We outperform all methods in terms of IS and CIS as well. Our method generates high variety translations, which is in line with our findings using our local style metric \mathbf{H}^k .

We conduct a user study on Amazon Mechanical Turk and ask the users which translation is closer to the exemplar in terms of color and appearance. We show the users one target image, and translations from the six methods in Fig. 4. 77 users participate in the study, each one evaluating 39 comparisons of 6 translations. In total, there are 90 translation-target pairs that were randomly chosen. Out of 3003 votes, our method received the most votes (1062), see Table 2. MUNIT [11] is the second best model with 860.



Figure 3. **Effect of the exemplar.** Our method can change the appearance of each semantic region differently, yet has realistic output.

GTA → CS	car	sky	vegetation	building	side-walk	road	Avg
MUNIT [11]	0.43	0.78	0.21	0.28	0.13	0.06	0.32
DRIT [18]	0.41	1.21	0.27	0.27	0.12	0.08	0.39
CUT [28]	0.44	0.92	0.24	0.36	0.16	0.13	0.38
FSeSim [42]	0.4	0.96	0.25	0.38	0.15	0.13	0.38
MGUIT [12]	0.45	1.42	0.29	0.39	0.18	0.19	0.49
Ours(DSI2I)	0.29	0.22	0.16	0.29	0.08	0.03	0.17
CS → GTA	car	sky	vegetation	building	side-walk	road	Avg
MUNIT [11]	0.57	0.44	0.59	0.53	0.47	0.35	0.49
DRIT [18]	0.66	0.63	0.53	0.56	0.51	0.39	0.55
CUT [28]	0.88	0.58	0.75	0.67	0.72	0.74	0.72
FSeSim [42]	0.77	0.68	0.75	0.75	0.70	0.63	0.71
MGUIT [12]	0.76	0.69	0.69	0.65	0.68	0.57	0.67
Ours(DSI2I)	0.35	0.17	0.44	0.41	0.50	0.29	0.36

Table 3. Comparison with other methods. Classwise stylistic distance between translation-exemplar pairs (lower is better).

Lastly, we measure the segmentation accuracy of pre-trained models with our translations, see the last column of Table 4. We use Cityscapes pretrained DRN for translations of GTA images and vice versa. Due to the perceptual losses, our method is good at preserving content.

4.4. Ablation Study

To understand the effect of dense style independently from the semantic correspondence, we use segmentation labels as $\frac{\mathbf{M}_y^T}{\mathbf{M}_{yy}^T} \mathbf{M}_x$ instead of \mathbf{A}_{yx} in Table 5. This is equivalent to averaging \mathbf{S}_y^{dense} class-wise and then swapping it between corresponding classes. Our ablations on 5 show that losses on \mathbf{S}_{mix} and \mathbf{S}_{glb} encourage our model to preserve content and generate high quality translations.

We assess the effectiveness of our semantic correspon-

GTA → CS	FID ↓	IS ↑	CIS ↑	Seg Acc ↑
MUNIT [11]	47.76	3.19	1.08	0.79
DRIT [18]	42.93	3.12	1.08	0.70
CUT [28]	50.89	3	1	0.62
FSeSim [42]	48.77	3.08	1	0.71
MGUIT [12]	44.36	2.88	1.03	0.65
Ours(DSI2I)	42.61	3.43	1.19	0.82
CS → GTA	FID ↓	IS ↑	CIS ↑	Seg Acc ↑
MUNIT [11]	48.91	3.56	1.17	0.79
DRIT [18]	48.18	3.82	1.17	0.72
CUT [28]	65.68	3.9	1	0.61
FSeSim [42]	64.81	4.4	1	0.74
MGUIT [12]	55.72	3.63	1.05	0.68
Ours(DSI2I)	45.12	3.85	1.36	0.81

Table 4. Fidelity and diversity of the translations. Our method outperforms all others on all metrics.

GTA → CS	FID ↓	Seg Acc ↑
Ours(DSI2I)	42.81	0.83
Ours(DSI2I) w/o S^{mix}	43.92	0.82
Ours(DSI2I) w/o S^{glb}	43.73	0.81
Ours(DSI2I) w/o S^{mix}, S^{glb}	45.67	0.78
CS → GTA	FID ↓	Seg Acc ↑
Ours(DSI2I)	44.75	0.81
Ours(DSI2I) w/o S^{mix}	46.15	0.79
Ours(DSI2I) w/o S^{glb}	46.71	0.78
Ours(DSI2I) w/o S^{mix}, S^{glb}	50.95	0.76

Table 5. Ablation study on S^{mix} and S^{glb} . The segmentation labels are used in the ablation study.

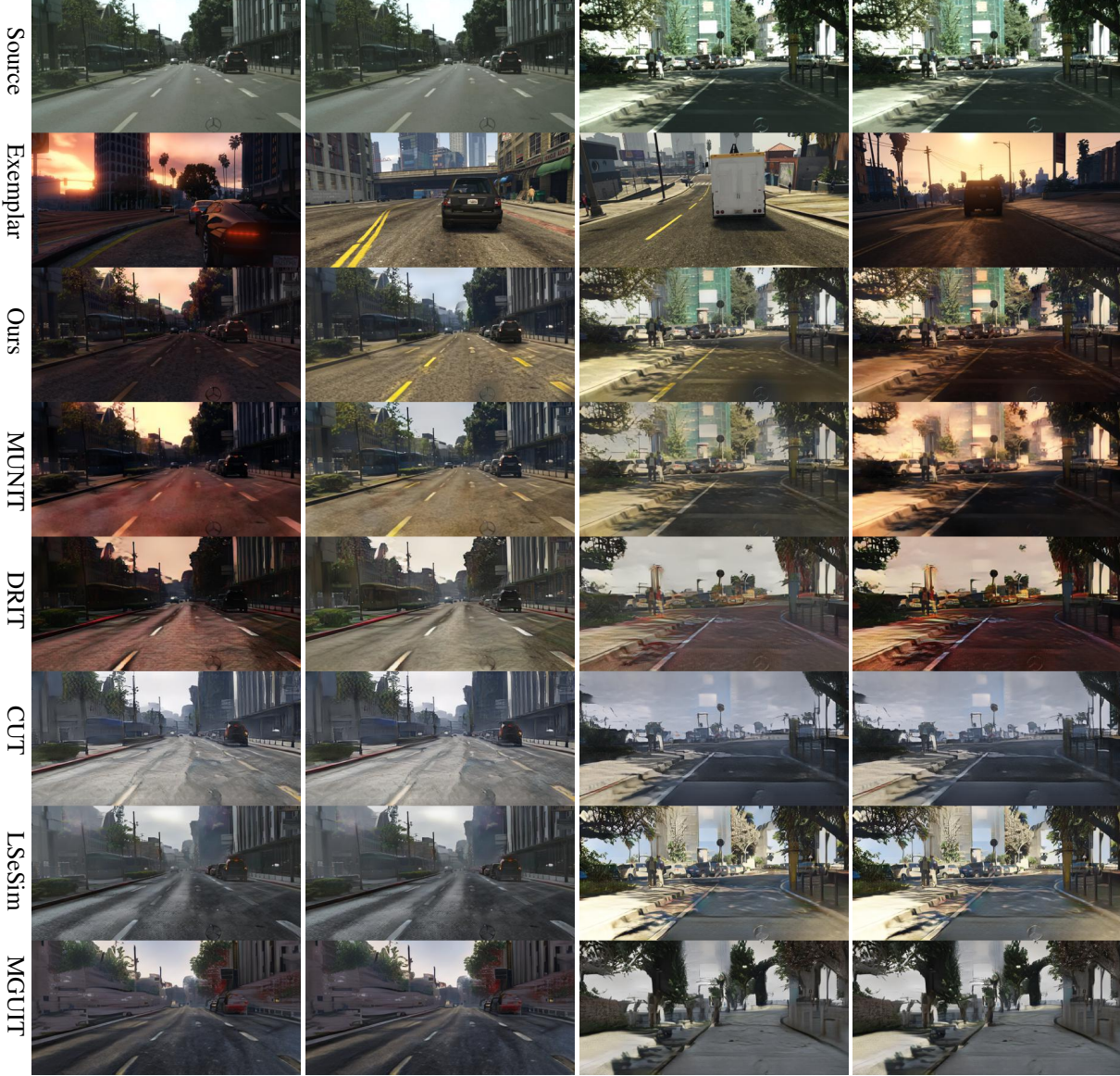


Figure 4. **Qualitative comparison with other methods.** In the first column, our method can disentangle road from sky and preserves the dark color for the road. In the second column, the appearance of the road and road lines in our translation are closest to those in the exemplar. In the last two columns, our model preserves the content semantics better, especially for tree and building classes.

Corr Acc	GTA \rightarrow CS	CS \rightarrow GTA
Ours	0.59	0.59
Ours w/o \mathbf{p}_y	0.57	0.56

Table 6. Accuracy of semantic correspondence. Our unsupervised \mathbf{p}_y increases the accuracy of correspondence.

dence module by setting \mathbf{p}_y as uniform distribution. Similar to warping \mathbb{S}_y^{dense} , we warp the segmentation labels \mathbb{M}_y and report the accuracy with the warped labels in Table 6. We observe a drop in the accuracy of the warped labels.

5. Conclusion

We present a framework for UEI2I that densely represents style and show how it can be learned and exchanged. This allows local stylistic changes of each semantic region. Our method does not require any labels. We quantitatively and qualitatively show the effectiveness of our method.

Acknowledgement. This work was supported in part by the Swiss National Science Foundation via the Sinergia grant CRSII5-180359. We also thank Ehsan Pajouheshgar for valuable discussions.

References

- [1] Kfir Aberman, Jing Liao, Mingyi Shi, Dani Lischinski, Baoquan Chen, and Daniel Cohen-Or. Neural best-buddies: Sparse cross-domain correspondence. *ACM Transactions on Graphics (TOG)*, 37(4):1–14, 2018. [3](#)
- [2] Connelly Barnes, Eli Shechtman, Adam Finkelstein, and Dan B Goldman. Patchmatch: A randomized correspondence algorithm for structural image editing. *ACM Trans. Graph.*, 28(3):24, 2009. [3](#)
- [3] Deblina Bhattacharjee, Seungryong Kim, Guillaume Vezier, and Mathieu Salzmann. Dunit: Detection-based unsupervised image-to-image translation. In *Proceedings of the IEEE/CVF Conference on Computer Vision and Pattern Recognition*, pages 4787–4796, 2020. [1, 2](#)
- [4] Tai-Yin Chiu and Danna Gurari. Photowct2: Compact autoencoder for photorealistic style transfer resulting from blockwise training and skip connections of high-frequency residuals. In *Proceedings of the IEEE/CVF Winter Conference on Applications of Computer Vision*, pages 2868–2877, 2022. [3](#)
- [5] Marius Cordts, Mohamed Omran, Sebastian Ramos, Timo Rehfeld, Markus Enzweiler, Rodrigo Benenson, Uwe Franke, Stefan Roth, and Bernt Schiele. The cityscapes dataset for semantic urban scene understanding. In *Proc. of the IEEE Conference on Computer Vision and Pattern Recognition (CVPR)*, 2016. [6](#)
- [6] Marco Cuturi. Sinkhorn distances: Lightspeed computation of optimal transport. *Advances in neural information processing systems*, 26, 2013. [1, 5](#)
- [7] Leon A Gatys, Alexander S Ecker, and Matthias Bethge. Image style transfer using convolutional neural networks. In *Proceedings of the IEEE conference on computer vision and pattern recognition*, pages 2414–2423, 2016. [3, 6](#)
- [8] Martin Heusel, Hubert Ramsauer, Thomas Unterthiner, Bernhard Nessler, and Sepp Hochreiter. Gans trained by a two time-scale update rule converge to a local nash equilibrium. *Advances in neural information processing systems*, 30, 2017. [6](#)
- [9] Xueqi Hu, Xinyue Zhou, Qiusheng Huang, Zhengyi Shi, Li Sun, and Qingli Li. Qs-attn: Query-selected attention for contrastive learning in i2i translation. In *Proceedings of the IEEE/CVF Conference on Computer Vision and Pattern Recognition*, pages 18291–18300, 2022. [2](#)
- [10] Xun Huang and Serge Belongie. Arbitrary style transfer in real-time with adaptive instance normalization. In *Proceedings of the IEEE international conference on computer vision*, pages 1501–1510, 2017. [3](#)
- [11] Xun Huang, Ming-Yu Liu, Serge Belongie, and Jan Kautz. Multimodal unsupervised image-to-image translation. In *Proceedings of the European conference on computer vision (ECCV)*, pages 172–189, 2018. [1, 2, 3, 5, 6, 7](#)
- [12] Somi Jeong, Youngjung Kim, Eunbeom Lee, and Kwanghoon Sohn. Memory-guided unsupervised image-to-image translation. In *Proceedings of the IEEE/CVF Conference on Computer Vision and Pattern Recognition*, pages 6558–6567, 2021. [1, 2, 7](#)
- [13] Chanyong Jung, Gihyun Kwon, and Jong Chul Ye. Exploring patch-wise semantic relation for contrastive learning in image-to-image translation tasks. In *Proceedings of the IEEE/CVF Conference on Computer Vision and Pattern Recognition*, pages 18260–18269, 2022. [2](#)
- [14] Tero Karras, Samuli Laine, and Timo Aila. A style-based generator architecture for generative adversarial networks. In *Proceedings of the IEEE/CVF conference on computer vision and pattern recognition*, pages 4401–4410, 2019. [5](#)
- [15] Soohyun Kim, Jongbeom Baek, Jihye Park, Gyeongnyeon Kim, and Seungryong Kim. Instformer: Instance-aware image-to-image translation with transformer. In *Proceedings of the IEEE/CVF Conference on Computer Vision and Pattern Recognition*, pages 18321–18331, 2022. [1, 2](#)
- [16] Sunnie SY Kim, Nicholas Kolkin, Jason Salavon, and Gregory Shakhnarovich. Deformable style transfer. In *European Conference on Computer Vision*, pages 246–261. Springer, 2020. [3](#)
- [17] Nicholas Kolkin, Jason Salavon, and Gregory Shakhnarovich. Style transfer by relaxed optimal transport and self-similarity. In *Proceedings of the IEEE/CVF Conference on Computer Vision and Pattern Recognition*, pages 10051–10060, 2019. [3, 6](#)
- [18] Hsin-Ying Lee, Hung-Yu Tseng, Jia-Bin Huang, Maneesh Singh, and Ming-Hsuan Yang. Diverse image-to-image translation via disentangled representations. In *Proceedings of the European conference on computer vision (ECCV)*, pages 35–51, 2018. [1, 2, 7](#)
- [19] Boyi Li, Felix Wu, Kilian Q Weinberger, and Serge Belongie. Positional normalization. In *Advances in Neural Information Processing Systems*, pages 1620–1632, 2019. [3, 4](#)
- [20] Yijun Li, Chen Fang, Jimei Yang, Zhaowen Wang, Xin Lu, and Ming-Hsuan Yang. Universal style transfer via feature transforms. *Advances in neural information processing systems*, 30, 2017. [3](#)
- [21] Yijun Li, Ming-Yu Liu, Xueting Li, Ming-Hsuan Yang, and Jan Kautz. A closed-form solution to photorealistic image stylization. In *Proceedings of the European Conference on Computer Vision (ECCV)*, pages 453–468, 2018. [3](#)
- [22] Yanghao Li, Naiyan Wang, Jiaying Liu, and Xiaodi Hou. Demystifying neural style transfer. *arXiv preprint arXiv:1701.01036*, 2017. [3, 6](#)
- [23] Ce Liu, Jenny Yuen, and Antonio Torralba. Sift flow: Dense correspondence across scenes and its applications. *IEEE transactions on pattern analysis and machine intelligence*, 33(5):978–994, 2010. [3](#)
- [24] Xiao-Chang Liu, Yong-Liang Yang, and Peter Hall. Learning to warp for style transfer. In *Proceedings of the IEEE/CVF Conference on Computer Vision and Pattern Recognition*, pages 3702–3711, 2021. [3](#)
- [25] Yanbin Liu, Linchao Zhu, Makoto Yamada, and Yi Yang. Semantic correspondence as an optimal transport problem. In *Proceedings of the IEEE/CVF Conference on Computer Vision and Pattern Recognition*, pages 4463–4472, 2020. [1, 3, 5](#)
- [26] Juhong Min, Jongmin Lee, Jean Ponce, and Minsu Cho. Hyperpixel flow: Semantic correspondence with multi-layer

- neural features. In *Proceedings of the IEEE/CVF International Conference on Computer Vision*, pages 3395–3404, 2019. 3
- [27] Sangwoo Mo, Minsu Cho, and Jinwoo Shin. Instagan: Instance-aware image-to-image translation. *arXiv preprint arXiv:1812.10889*, 2018. 2
- [28] Taesung Park, Alexei A Efros, Richard Zhang, and Jun-Yan Zhu. Contrastive learning for unpaired image-to-image translation. In *European conference on computer vision*, pages 319–345. Springer, 2020. 2, 7
- [29] Taesung Park, Ming-Yu Liu, Ting-Chun Wang, and Jun-Yan Zhu. Semantic image synthesis with spatially-adaptive normalization. In *Proceedings of the IEEE Conference on Computer Vision and Pattern Recognition*, 2019. 3
- [30] Alec Radford, Jong Wook Kim, Chris Hallacy, Aditya Ramesh, Gabriel Goh, Sandhini Agarwal, Girish Sastry, Amanda Askell, Pamela Mishkin, Jack Clark, et al. Learning transferable visual models from natural language supervision. In *International Conference on Machine Learning*, pages 8748–8763. PMLR, 2021. 1, 5
- [31] Stephan R. Richter, Vibhav Vineet, Stefan Roth, and Vladlen Koltun. Playing for data: Ground truth from computer games. In Bastian Leibe, Jiri Matas, Nicu Sebe, and Max Welling, editors, *European Conference on Computer Vision (ECCV)*, volume 9906 of *LNCS*, pages 102–118. Springer International Publishing, 2016. 6
- [32] Tim Salimans, Ian Goodfellow, Wojciech Zaremba, Vicki Cheung, Alec Radford, and Xi Chen. Improved techniques for training gans. *Advances in neural information processing systems*, 29, 2016. 6
- [33] Zhiqiang Shen, Mingyang Huang, Jianping Shi, Xiangyang Xue, and Thomas S Huang. Towards instance-level image-to-image translation. In *Proceedings of the IEEE/CVF conference on computer vision and pattern recognition*, pages 3683–3692, 2019. 1, 2
- [34] Karen Simonyan and Andrew Zisserman. Very deep convolutional networks for large-scale image recognition. *arXiv preprint arXiv:1409.1556*, 2014. 3
- [35] Jinchao Yang, Fei Guo, Shuo Chen, Jun Li, and Jian Yang. Industrial style transfer with large-scale geometric warping and content preservation. In *Proceedings of the IEEE/CVF Conference on Computer Vision and Pattern Recognition*, pages 7834–7843, 2022. 3
- [36] Jaejun Yoo, Youngjung Uh, Sanghyuk Chun, Byeongkyu Kang, and Jung-Woo Ha. Photorealistic style transfer via wavelet transforms. In *Proceedings of the IEEE/CVF International Conference on Computer Vision*, pages 9036–9045, 2019. 3
- [37] Fisher Yu, Vladlen Koltun, and Thomas Funkhouser. Dilated residual networks. In *Proceedings of the IEEE conference on computer vision and pattern recognition*, pages 472–480, 2017. 6
- [38] Fangneng Zhan, Yingchen Yu, Kaiwen Cui, Gongjie Zhang, Shijian Lu, Jianxiong Pan, Changgong Zhang, Feiying Ma, Xuansong Xie, and Chunyan Miao. Unbalanced feature transport for exemplar-based image translation. In *Proceedings of the IEEE/CVF Conference on Computer Vision and Pattern Recognition*, pages 15028–15038, 2021. 3
- [39] Fangneng Zhan, Yingchen Yu, Rongliang Wu, Jiahui Zhang, Shijian Lu, and Changgong Zhang. Marginal contrastive correspondence for guided image generation. In *Proceedings of the IEEE/CVF Conference on Computer Vision and Pattern Recognition*, pages 10663–10672, 2022. 3
- [40] Pan Zhang, Bo Zhang, Dong Chen, Lu Yuan, and Fang Wen. Cross-domain correspondence learning for exemplar-based image translation. In *Proceedings of the IEEE/CVF Conference on Computer Vision and Pattern Recognition*, pages 5143–5153, 2020. 3, 5
- [41] Yulun Zhang, Chen Fang, Yilin Wang, Zhaowen Wang, Zhe Lin, Yun Fu, and Jimei Yang. Multimodal style transfer via graph cuts. In *Proceedings of the IEEE/CVF International Conference on Computer Vision*, pages 5943–5951, 2019. 3
- [42] Chuanxia Zheng, Tat-Jen Cham, and Jianfei Cai. The spatially-correlative loss for various image translation tasks. In *Proceedings of the IEEE/CVF Conference on Computer Vision and Pattern Recognition*, pages 16407–16417, 2021. 2, 7
- [43] Xingran Zhou, Bo Zhang, Ting Zhang, Pan Zhang, Jianmin Bao, Dong Chen, Zhongfei Zhang, and Fang Wen. Cocosnet v2: Full-resolution correspondence learning for image translation. In *Proceedings of the IEEE/CVF Conference on Computer Vision and Pattern Recognition*, pages 11465–11475, 2021. 3
- [44] Jun-Yan Zhu, Taesung Park, Phillip Isola, and Alexei A Efros. Unpaired image-to-image translation using cycle-consistent adversarial networks. In *Proceedings of the IEEE international conference on computer vision*, pages 2223–2232, 2017. 2
- [45] Peihao Zhu, Rameen Abdal, Yipeng Qin, and Peter Wonka. Sean: Image synthesis with semantic region-adaptive normalization. In *Proceedings of the IEEE/CVF Conference on Computer Vision and Pattern Recognition*, pages 5104–5113, 2020. 3